arXiv:cond-mat/9603087v1 12 Mar 1996

Fluid Induced Particle Size Segregation in Sheared Granular Assemblies

Sitangshu Bikas Santra[1], Stefan Schwarzer,[1,2*]
and Hans Herrmann[1,2]
[1] *Laboratoire de Physique Mécanique des Milieux Hétérogènes,*
Ecole Supérieure de Physique et Chimie Industrielles, 75231 Paris, Cedex 05, France
[2] *Institut für Computeranwendungen, Universität Stuttgart,*
Pfaffenwaldring 27, 70569 Stuttgart, Germany
(February 1, 2008)

Abstract

We perform a two-dimensional molecular-dynamics study of a model for sheared bidisperse granular systems under conditions of simple shear and Poiseuille flow. We propose a mechanism for particle-size segregation based on the observation that segregation occurs if the viscous length scale introduced by a liquid in the system is smaller than of the order of the particle size. We show that the ratio of shear rate to viscosity must be small if one wants to find size segregation. In this case the particles in the system arrange themselves in bands of big and small particles oriented along the direction of the flow. Similarly, in Poiseuille flow we find the formation of particle bands. Here, in addition, the variety of time scales in the flow leads to an aggregation of particles in the zones of low shear rate and can suppress size segregation in these regions. The results have been verified against simulations using a full Navier-Stokes description for the liquid.

PACS numbers: 83.20.Hn, 47.55.Kf, 02.70.Ns

Typeset using REVTEX

I. INTRODUCTION

If a mixture of particles and liquid is sheared, either in a continuous fashion or by periodic excitation of the system, a host of structural rearrangements in the mixture are known to occur. Most of the systems studied experimentally involve mono-disperse suspensions [1–3]. For concentrated suspensions and oscillatory shearing the formation of layers in the iso-velocity planes and an additional arrangement in lines of particles perpendicular to the velocity field [3] has been observed. In addition, simulations of Taylor-Couette flow in the viscous regime confirm the organization of the particles in the suspension in layers oriented along the iso-velocity planes [4]. Numerically, cluster formation has been found in these simulations within the formed planes. Although for bidisperse suspensions similar organization patterns have been found [3] and size-distribution induced instabilities have been observed in sedimentation experiments [5], simulations here so far have not found clear indications of size segregation under shear.

In this paper, we want to investigate particle size segregation of a granular medium under shear flow conditions in two dimensions in the presence of a liquid. The mechanism for size segregation in this model is basically of geometric nature and may generalize to three dimensions. We concentrate on pipe and laminar shear flows described by local shear rates $\dot{\gamma} \equiv (\partial/\partial y)v_x$, where we have in mind (see Fig. 1) that the flow is translationally invariant in x direction and that its speed varies in y direction.

II. THE MODEL

For the sake of simplicity we assume the particle size distribution to be bidisperse, i.e., our system consists of a number n_s of small and a number n_b of big disk shaped particles with radii r_s and r_b, respectively. These particles are initially distributed randomly over a two dimensional plane with a specified area fraction c. The overall area fraction c is the sum of the area fractions of big and small particles, $c = c_s + c_b$. Under viscous conditions and when two particles are nearly in contact, lubrication effects will introduce a strong velocity dependent damping that inhibits particle collisions. In our model, we allow for small particle overlaps, but between overlapping particles strong repulsive forces and and a velocity proportional damping are introduced. I.e, in normal direction acts a damped harmonic force f_n,

$$f_n = -\mu\xi + 2\mu\kappa v_n, \tag{1}$$

where μ is the reduced mass of the pair, $\xi \equiv |\mathbf{x}_1 - \mathbf{x}_2| - (r_1 + r_2)$ is the virtual overlap of the two particles located at $\mathbf{x}_1$ and $\mathbf{x}_2$ (Fig. 2), v_n is the normal component of the relative velocity, and κ parameterizes a velocity proportional damping. The form of Eq. (1) is such that the *restitution coefficient* e, the ratio of the normal velocities after and before the impact, is the same for all binary collisions, independent of mass and velocity. The restitution e is related to κ by $\kappa \equiv 1/\sqrt{1 + (\pi/\log(e))^2}$ and is chosen to be 0.8 in this work. Equation (1) is in dimensionless form, the chosen length scale is the average radius $\bar{r} \equiv (n_b r_b + n_s r_s)/(n_b + n_s)$, the mass unit is the mass of a particle of average radius, and the time unit is such that the "spring constant" of a pair contact becomes unity and thus

does not appear in Eq. (1). More precisely, in these units an elastic contact with $\kappa = 0$ has a duration of π. We neglect tangential forces in our model and consequently we do not consider particle rotation. The equations of motion are integrated using a fourth order Gear predictor-corrector algorithm, with the time step chosen to be 0.15, which still guarantees good energy conservation in the elastic case.

To prepare the initial configuration, we start from a random configuration of disks and simulate with periodic boundary conditions until time $t = 20$ using a very low restitution coefficient of 0.1 to remove particle overlaps and excess energy in the system efficiently. Afterwards the setup is continued with $e = 1$ until $t = 100$, corresponding to elastic collisions. The average energy per particle in the system during this stage is quite low and allows only marginal overlaps. Thus, the resulting configuration is close to that of a hard disk system in thermal equilibrium.

The liquid motion is approximated by an invariant velocity field in x direction,

$$\mathbf{u}(y) = y\dot{\gamma}\mathbf{e}_x, \tag{2}$$

where y is counted from the center of the simulation cell (cf. Fig 1). We have tested the implicit assumption that the velocity profile is stationary for shear flow, i.e., that it is not modified by the presence of the particles in the fluid [6]. It differs only little from the theoretical constant viscosity profile in the case of Poiseuille flow as shown later in this article.

The liquid exerts an additional drag on each particle i which is added to the interaction force (1) between particles. The force is here assumed to be the Stokes drag force on a sphere,

$$\mathbf{f}_{d,i} = -6\pi r_i \eta \left[\mathbf{v}_i - \mathbf{u}(y_i)\right], \tag{3}$$

where $\mathbf{v}_i$ is the velocity of particle i and y_i its y coordinate.

We then start the simulation by choosing the initial particle velocities to be equal to the local liquid-background velocity. The boundary conditions for the particles are Lees-Edwards boundary conditions (as displayed in Fig. 1, cf. also [7]) with shear rate $\dot{\gamma}$.

III. RESULTS OF THE SHEAR FLOW CASE

In Figs. 3 and 4 we show two typical simulation sequences whose physical parameters differ only in the value for the background viscosity η. The ratio of the particle radii in our bidisperse system is $r_b/r_s = 4$, the ratio of the number density of big and small particles is $n_b/n_s = 0.05$ and the total area fraction of particles is rather high, $c = 0.6$. In the long time limit one sees very different structural reordering of the systems emerging. In the first sequence (Fig. 3) with low viscosity, the particle arrangement is more or less random, whereas in the second case (Fig. 4) one observes a very clear separation into alternating zones parallel to the flow direction which contain alternatingly big and small particles, respectively.

The basis to understand this segregation phenomenon lies in an analysis of the length scales that are present in the system. Apart from the system size and the two different particle radii an additional viscous length exists in the problem. Given that a particle has

a typical particular velocity against the liquid background of $\mathbf{v}_0$ — which it acquires in collisions, see below — the viscous length ζ is the typical distance that a particle has to travel before it again acquires the velocity of the background. The length ζ may be estimated in the following way. From the equations of motion $\mathbf{f}_{d,i} = m_i\dot{\mathbf{v}}$, i.e.,

$$\dot{v}_y = -\frac{6\pi r_i \eta}{m_i} v_y, \tag{4}$$

we obtain a simple exponential decay of any excess residual y component of the velocity,

$$v_y(t) = v_0 \exp\left[-\frac{6\pi r_i \eta}{m_i} t\right]. \tag{5}$$

with a time constant $\tau = m_i/6\pi r_i\eta$. A typical excess velocity v_0 created by a collision of two particles 1 and 2 is $v_0 \approx (\mu/m_i)(r_1 + r_2)\dot{\gamma}$. The product

$$\zeta_1 \approx v_0\tau = \mu(1 + r_2/r_1)\dot{\gamma}/6\pi\eta \tag{6}$$

estimates the viscous length for particle type 1 after a collision with a type 2 particle. The value of ζ_1 is largest for $r_2/r_1 = r_b/r_s$ and we call it simply ζ in the subsequent text. A detailed discussion is presented in App. A.

We propose the following physical picture of the segregation process: The particles move on average with the velocity of the liquid at their centers. The collisions between particles tend to drive the system to a state of a random particle distribution [8]. The ratio of the viscous length to a typical inter-particle distance is a measure for the efficiency of this process — the larger the viscous length, the more effectively will a collision disperse the state of the system. Conversely however, in a highly viscous environment with $\zeta \ll 1$, collisions will create order.

To see the involved mechanism let us first look for stationary states of a monodisperse system, which we will define as those states not leading to particle displacements in y-direction of more than half a particle diameter. Each single particle defines, due to its finite extension, a horizontal "lane" in the system, i.e., the area that would be covered as time passes if no other particles were present in the system. A second particle will undergo collisions with the first particle if (i) their lanes overlap and (ii) if their y-coordinates differ — under periodic boundary conditions the particles cannot escape each other.

For a finite system with a given height one can find a maximum particle concentration below which all particles can be in disjoint lanes. But for an infinite system this concentration tends to zero, since collisions will necessarily occur if the particle arrangements are random. On the condition that the particle area fraction does not exceed the maximum packing fraction of disks in a strip one diameter wide, $c_0 \equiv \pi/4$, we can imagine a stationary, collisionless configuration of particles. Let the particles be arranged one after another in a horizontal lane, all with the same y-coordinate. Then let these lanes be stacked in y-direction. Varying the horizontal distances between particles and the vertical distances between lanes any concentration $c \leq c_0$ can be achieved.

Such a particle arrangement seems to be highly singular, but it can under certain conditions be stable against perturbations. Let the vertical distance between lanes be small with respect to $r = 1$ and imagine one particle in one of the lanes being slightly displaced

in $+y$-direction. The particle will either undergo a collision with another particle in the lane above, which will then reduce its y-coordinate again, or it will collide with a particle in its own lane, increasing the original displacement. If the viscous length ζ is large ($\gg 1$), this collision may suffice to displace both collision partners to another lane (if at the same time also the mean free path is large enough, see App. B). In contrast, if ζ is small ($\ll 1$), then the relative motion of the two particles is more akin to a sliding on top of each other, displacing each particle by $\approx 1/2$ in $+y$ and $-y$-direction respectively. In a sufficiently dense system subsequent collisions with particles can the neighboring lanes can then restore the original vertical positions of the particles.

In the polydisperse case we might now expect that mixed lanes, containing both big and small particles, are stable. However, arguments can be made against this supposition. If ζ is small in comparison to the big particle radius then small particles in lanes containing big particles will be ejected from the big particle lane by collisions. The reason is that the big massive collision partner is not significantly displaced by one collision, whereas the small partner is. If then the neighboring lane contains small particles, it is not hard to absorb the additional expelled particle. If, however, the neighboring lane contains big particles, alternating collision series of the small particle with big particles below and above will establish an additional small particle lane in between the big particle lanes.

Starting from a random configuration at small ζ, local groups of big particles will tend to align and expel small particles — neighboring groups may then join due to the stresses generated by the collisions with the small particles accumulating outside these groups. Finally, stable lanes form segregates into a of particles in disjoint lanes. A typical simulation sequence of this ordering process is displayed in Fig. 4.

To arrive at a quantitative description of the segregation process, we define an "order parameter" in the following way. Since we have observed a strong stratification of the flow into horizontal layers, we define for each particle species the area fraction in a horizontal strip of width of the average particle radius. For a completely segregated system, we expect the area fraction of small particles a_s to be large whenever the fraction of big particles a_b is small. Consequently, the quantity

$$\delta \equiv \langle [a_b - a_s - \langle a_b - a_s \rangle]^2 \rangle^{1/2} \tag{7}$$

is small for a random mixture of the two species and assumes a large value when the system is stratified. The brackets denote the average over all examined horizontal slices.

In Fig. 5 we show the time dependence of δ for different values of ζ for constant overall area fraction $c = 0.6$ and constant shear rate $\dot{\gamma} = 0.01$. We clearly see an initially fast size segregation process which becomes slower and slower and finally saturates to a value δ_∞ that depends on ζ. Due to the rather low value of ζ and consequently a strong non-ergodicity of our systems, the sample-to-sample fluctuations are large and values of $0.2\delta_\infty$ are typical in samples of size 100×100.

The decreasing dependence of δ_∞ on ζ, which demonstrates the mixing or destabilizing effects of large ζ, is shown in Fig. 6. The figure shows data obtained for different fluid viscosities and shear rates $\dot{\gamma}$, but constant overall area fraction. The scatter is rather large due to the abovementioned sample-to-sample fluctuations. At large ζ, the segregation does not increase significantly over the initial value. In fact, if ζ is larger than the mean free path between particles, then the spatial distribution of particles does not differ much from that of

the corresponding, inelastic, sheared hard-core gas [9]. However, at small ζ the friction with the liquid is very large and causes ordering in bands oriented parallel to the flow containing alternatingly big and small particles. For a proposal to scale not only with respect to $\dot{\gamma}$ and η but also incorporating the concentration c, see App. B.

IV. POISEUILLE FLOW

To see the influence on the ordering effect of a different flow profile, we have exchanged the simple linear shear profile of Eq. (2) by a quadratic Poiseuille profile,

$$\mathbf{u}(y) = 4L(\frac{y}{L} + \frac{1}{2})(\frac{y}{L} - \frac{1}{2})v_{\max}\mathbf{e}_x. \tag{8}$$

We keep periodic boundary conditions in x-direction while introducing reflecting walls at the bottom and the top of the cell, where the flow velocity is zero in accord with no-slip boundary conditions. The shear rate now depends on the y-coordinate in the flow,

$$\dot{\gamma}_y = 8\frac{y}{L}v_{\max}. \tag{9}$$

Its modulus $|(\partial/\partial y)v_x|$ is largest at the walls and zero in the center of the flow.

We have studied systems of concentration $c = 0.6$ and $c = 0.4$ with viscosity $\eta = 0.01$ and shear rates of $\dot{\gamma}_{L/4} = 0.01$ at $y = L/4$ so that a typical zone in the flow corresponds to the crossover regime where $\zeta \approx 1$. After a long time $t\dot{\gamma}_{L/4} \approx 100$ we find that the particles concentrate in the central region of the cell, where the shear rate is smallest, cf. Fig. 7. Close to the wall, and although the shear is largest there, we still find stratification — small particles gather at the wall.

In a real experimental system, the liquid is strongly coupled to the particles. The momentum exchange between the two phases alters significantly the flow pattern, both on the scale of the particle radius, but at least in the viscous regime also on the scale of the container. We have tested our assumption of a laminar profile on the scale of the container by comparison to the results of a newly developed algorithm whose details are described in Refs. [10,11]. There, we couple the particles to the liquid by Stokes-type drag forces proportional to the particle radius and the local velocity difference to the flow field — corresponding to Eq. (3). The drag is introduced as a point-force term in the Navier-Stokes equations for the liquid surrounding the particles and accounts for the momentum transfer from the particles to the liquid. The Navier-Stokes equation is solved by a finite difference scheme, where the grid has a resolution on the order of the particle size. This technique is appropriate to observe the long range effects of the hydrodynamic interaction between the particles. The result of this simulation is shown in Fig. 8, for the same choice of parameters as for the fixed velocity profile.

Since there is no drastic visible difference to the fixed profile calculation shown in Fig. 7(b) with the same physical parameters, we have *a posteriori* justified the choice a fixed liquid profile. To be more quantitative, we have checked the velocity profile of the combined particle-liquid system against the theoretical expectation for laminar liquid-only flow (see Fig. 9) with constant viscosity. For moderate Reynolds numbers (≈ 100) we find that there are only very small deviations from a parabolic flow profile. However, the particle load

increases the effective viscosity of the mixture and thus the overall flow velocity is reduced in comparison to the case of the pure liquid. In Fig. 9 we recognize a slight flattening of the parabolic profile near the center of the flow. Such a behavior is characteristic for shear thinning liquids and is here caused by the locally increased viscosity in the flow center, corresponding to the increased vertical momentum transport in the denser central region. At these Reynolds numbers, we measure only small velocity fluctuations of the liquid along the horizontal direction, i.e., the profile is stationary.

V. CONCLUSION

We have studied sheared bidisperse granular systems under conditions of simple shear and Poiseuille flow. We find that the presence of the liquid can induce particle size segregation. The criterion to decide whether this segregation mechanism will occur is that the ratio of shear rate to viscosity must be small. This statement is equivalent to saying that the viscous length in the system should be small when compared to a typical linear scale in the problem as, e.g., the particle radius. The particles arrange themselves in bands moving with the flow that contain alternatingly big and small particles.

Also in Poiseuille flow we observe the formation of bands of particles of different size. Here, in addition, the variety of time scales in the flow leads to an aggregation of particles in the zones of low shear rate. These results have been verified against simulations using a full Navier-Stokes simulation for the liquid.

The proposed segregation mechanism relies on the presence of a liquid phase. It is thus very different from known mechanisms in dry granular media, where gravity induced avalanches occur and separate particles species whose static angles of repose differ.

It should be very interesting to study the behavior of the system with more than two particle species or a whole continuum of species or the dependence on the particle radius ratio. Moreover, three dimensional calculations are desirable and quantitative comparisons to experiments are necessary.

VI. ACKNOWLEDGMENTS

We would like to thank in particular Stephane Roux for valuable suggestions. St. S. thanks Wolfgang Kalthoff and Stefan Luding for discussions. We thank the Höchleistungsrechenzentrum of the Forschungszentrum Jülich for computer time on their Paragon parallel computer. St. S. has been supported by a scholarship from the scientific council of NATO, granted by the Deutscher Akademischer Austauschdienst, Bonn.

APPENDIX A: VISCOUS LENGTH

We obtain an estimate (when no further collisions occur) for ζ by integration of the equations of motion $\mathbf{f}_{d,i} = m_i \dot{\mathbf{v}}$. Taking the drag force from Eq. (3), we have obtained for the y component of the equation of motion (4), which we print here once more:

$$\dot{v}_y = -\frac{6\pi r_i \eta}{m_i} v_y. \tag{A1}$$

This relation leads to a simple exponential relaxation of the initial excess velocity $v_y(0)$,

$$v_y(t) = v_y(0) \exp\left[-\frac{6\pi r_i \eta}{m_i} t\right]. \tag{A2}$$

In analogous fashion, we obtain the expression for the x component,

$$\dot{v}_x = -\frac{6\pi r_i \eta}{m_i}\left[v_x - \dot{\gamma}\int_0^t dt'\ v_y(t')\right], \tag{A3}$$

which we can integrate by standard methods to find $v_x(t)$. We define the viscous length as the norm of the vector valued integral

$$\zeta = \left\| \int_0^\infty dt\ \left[\mathbf{v}(t) - \mathbf{u}(y(t))\right] \right\| \tag{A4}$$

and use the solutions of (A1) and (A3) to obtain,

$$\zeta = \frac{m_i}{6\pi r_i \eta} \left\| \begin{pmatrix} v_x(0) - \frac{\dot{\gamma} m_i v_y(0)}{6\pi r_i \eta} \\ v_y(0) \end{pmatrix} \right\|. \tag{A5}$$

We then find typical values for $\mathbf{v}_0$ by a consideration of a two particle collision — say between particles with label 1 and 2 — assuming that the initial velocities equal $\mathbf{v}_i = \mathbf{u}(y_i)$ according to their different y positions in the flow (for a more complete discussion of inelastic two particle collisions, see, e.g. [12]). The velocities after the collision, in the reference frame comoving with the liquid at the initial position of particle 1, are

$$\mathbf{v}_1(0) = -\frac{\mu}{m_i} b\dot{\gamma} \begin{pmatrix} \sin\alpha\cos\alpha(1+e) \\ \sin^2\alpha - e\cos^2\alpha + 1 \end{pmatrix}. \tag{A6}$$

Here, b denotes the impact parameter and $\sin\alpha \equiv b/(r_1 + r_2)$, cf. Fig. 2. Thus, apart from order-one geometrical factors and some e dependence, the velocity of the scattered particle is [13] $\approx (\mu/m_i)(r_1 + r_2)\dot{\gamma}$. Therefore, ζ becomes largest for the small particles after a collision involving a big and a small particle:

$$\zeta \approx \frac{\mu(1 + r_b/r_s)\dot{\gamma}}{6\pi\eta}. \tag{A7}$$

APPENDIX B: AN ESTIMATE FOR THE MEAN FREE PATH IN THE MONODISPERSE SYSTEM

The ratio of the viscous length to the mean free path of the particles in a non-viscous environment is probably an important dynamical characteristics of the system. If the mean free free path is much shorter than the viscous length, the additional background viscosity will not have a big effect. If on the other hand the mean free path is much longer than the viscous length, then the behavior of the system is viscosity dominated. Here, we would like to give an estimate of the mean free path in a monodisperse system for particles moving in the vertical direction. To allow for a simple calculation in the stationary situation, we

resort to a simple hypotheses for the system's configuration at large times: due to the initial disorder the systems arranges itself such that the number of horizontal particle lanes is maximum.

We note that under these circumstances the average horizontal distance d between two particles is set by the packing fraction. If the number of lanes is maximum, their width must be the smallest possible, namely $2r$. One particle covers an area of πr^2 within the available area $2rd$. Consequently, the overall area fraction is

$$c = \frac{\pi r^2}{2rd} = \frac{1}{2}\pi\frac{r}{d}. \tag{B1}$$

As in the previous section, we now assume that we perturb the trajectory of one particle by giving it a vertical velocity of order $r\dot{\gamma}$, which is of the same order as the velocity difference between two lanes $2r\dot{\gamma}$. If $d = 2r$, the system will not allow particles to penetrate into the neighboring lane. This situation is the densest packing compatible with a stationary state of the system, $c_0 = \pi/4$. As long as $d < 4r$, or equivalently, $c > c_1 = \pi/8$, a particle will only occasionally be able to pass a lane. Considerations of the particle geometry apart, the probability for a hit should be proportional to the time spend in the lane by the scattered particle divided by the average time between the pass of two successive particles in the neighbor lane. The mean free path ℓ is given by the condition that this ratio be about 1, i.e.,

$$1 \approx \frac{\ell/\dot{\gamma}r}{(d-2r)/2\dot{\gamma}r,} \tag{B2}$$

or,

$$\ell/r \approx (d-2r)/2r = \frac{1}{4}\pi c^{-1} - 1 = \frac{c_0}{c} - 1. \tag{B3}$$

For even lower concentration, the particle has a good chance to pass one or even several lanes, each with probability $1 - p_{\rm hit} \approx 1 - [2r/\dot{\gamma}r]/[(d-2r)/2\dot{\gamma}r] = 1 - (2r)/(d-2r)$. The probability to survive a distance x/r without hits is hence distributed exponentially,

$$p(x/r) \sim (1 - p_{\rm hit})^{x/2r}, \tag{B4}$$

which yields — by normalization and determination of the expectation value —

$$\ell/r = -1/\ln(1 - p_{\rm hit}). \tag{B5}$$

For small concentrations (and thus also small hitting probabilities) this equation may be expanded to yield the same form as (B3)

$$\ell/r \sim 1/p_{\rm hit} \sim \frac{c_0}{c} - 1. \tag{B6}$$

It is interesting to note that ℓ does not depend on the shear rate but only on geometrical properties of the system. This observation is in favor of our suggestion that the ratio of viscous length to particle radius ζ/r, as proposed in the main text and here in dimensional form, collapses the simulation data for δ at a fixed given c. If $\dot{\gamma} \ll 1$, we presume that ζ/ℓ may be a good scaling variable, even at different area fractions. This may be an interesting question to investigate.

REFERENCES

* E-Mail: sts@ica1.uni-stuttgart.de

[1] B. Noetinger, L. Petit, E. Guazelli, and M. Clement, Rev. Phys. Appl. **22**, 1025 (1987).
[2] B. J. Ackerson and P. N. Pusey, Phys. Rev. Lett. **61**, 1033 (1988).
[3] P. Gondret, Ph.D. thesis, Université Claude Bernard, Lyon I, Lyon, 1994.
[4] G. Bossis and J. F. Brady, J. Chem. Phys. **80**, 5141 (1984).
[5] R. L. Whitmore, Br. J. Appl. Phys. **6**, 239 (1955).
[6] Of course the flow will differ on the scale of a single particle — we mean here that the flow remains unaltered on the scale of several particle sizes.
[7] M. P. Allen and D. J. Tildesley, *Computer Simulations of Liquids* (Clarendon Press, Oxford, 1987).
[8] The particle distribution will not become truely random, because dissipative systems form particle "clusters" [14] and in the elastic case the system heats up due to the applied shear and will have a particle distribution close to that of the hard-core gas.
[9] I. Goldhirsch and M.-L. Tan, (unpublished).
[10] W. Kalthoff, S. Schwarzer, G. Ristow, and H. Herrmann, submitted to Phys. Fluids [cond-mat 9501128] (unpublished).
[11] S. Schwarzer, Phys. Rev. E **52**, 6461 (1995).
[12] O. R. Walton, in *Particulate Two-Phase Flow*, edited by M. C. Roco (Butterworth-Heinemann, Boston, 1992), Chap. 25.
[13] We would like to point out that even in more elaborated models, which may include a more realistic rendering of the hydrodynamic interaction between the particles, the relevant velocity scale is of order $b\dot{\gamma}$ so that the following arguments remain valid.
[14] I. Goldhirsch and G. Zanetti, Phys. Rev. Lett. **70**, 1619 (1993).

FIGURES

FIG. 1. Sketch of the model geometry for shear flow. The simulation cell of size $L \times L$ is repeated in x-direction (periodic boundaries). The cell images in $\pm y$-direction are shifted by an amount of $\pm\dot{\gamma}Lt/2$ to reflect the particle displacement at the top and bottom of the cell which grows linearly in time due to the shear (Lees-Edward boundary condition).

FIG. 2. Geometry of the collision between two disks in the center of mass frame. The particles are assumed to initially move parallel to the flow, such that laboratory from and center of mass frame are aligned.

FIG. 3. Simulation snapshots at non-dimensional time $\dot{\gamma}t = 0$ (a) and 195 (b). The shear rate in this system is $\dot{\gamma} = 0.01$, the viscosity $\eta = 0.001$.

FIG. 4. Simulation snapshots at non-dimensional time $\dot{\gamma}t = 0$ (a), 20 (b), 70 (c), 110 (d) and 220 (e). The shear rate in this system is $\dot{\gamma} = 0.01$, the viscosity $\eta = 0.01$, ten times larger than in the preceding figure. Different shades of grey indicate the modulus of the x-velocity of the particles.

FIG. 5. Time dependence of the segregation parameter δ for simulations with different viscosity $\eta = 0.001,\ 0.004,\ 0.01,\ 0.03$ (bottom to top) corresponding to $\zeta \approx 2.5,\ 0.63,\ 0.25,\ 0.08$ [according to Eq. (A7)] (bottom curve to top curve) vs. dimensionless time $\dot{\gamma}t$ on the abscissa.

FIG. 6. Final values of the segregation parameter δ plotted vs. viscous length ζ [according to Eq. (A7)] on the abscissa for several values of viscosity and shear rate in the system. Crosses denote computations with constant viscosity $\eta = 0.01$, diamonds indicate constant shear rate $\dot{\gamma} = 0.01$.

FIG. 7. Stationary particle configuration with imposed parabolic Poiseuille flow profile. The system size is 100×100, the particle volume fraction $c = 0.4$ (a), and 0.6 (b).

FIG. 8. Final particle configuration in Poiseuille flow with velocity profile obtained by solution of the full Navier-Stokes equation with a point force term modeling the momentum exchange between fluid and particle phase. There is no difference in the physical parameters of the two systems. The system size is 80×40.

FIG. 9. The x-component of the velocity profile along a cut in y-direction in the Navier-Stokes Poiseuille flow simulation at $\mathrm{Re} = 100$. The solid line is the prediction for laminar flow without particles, the dashed line is a parabolic fit to the data points.

FIGURES

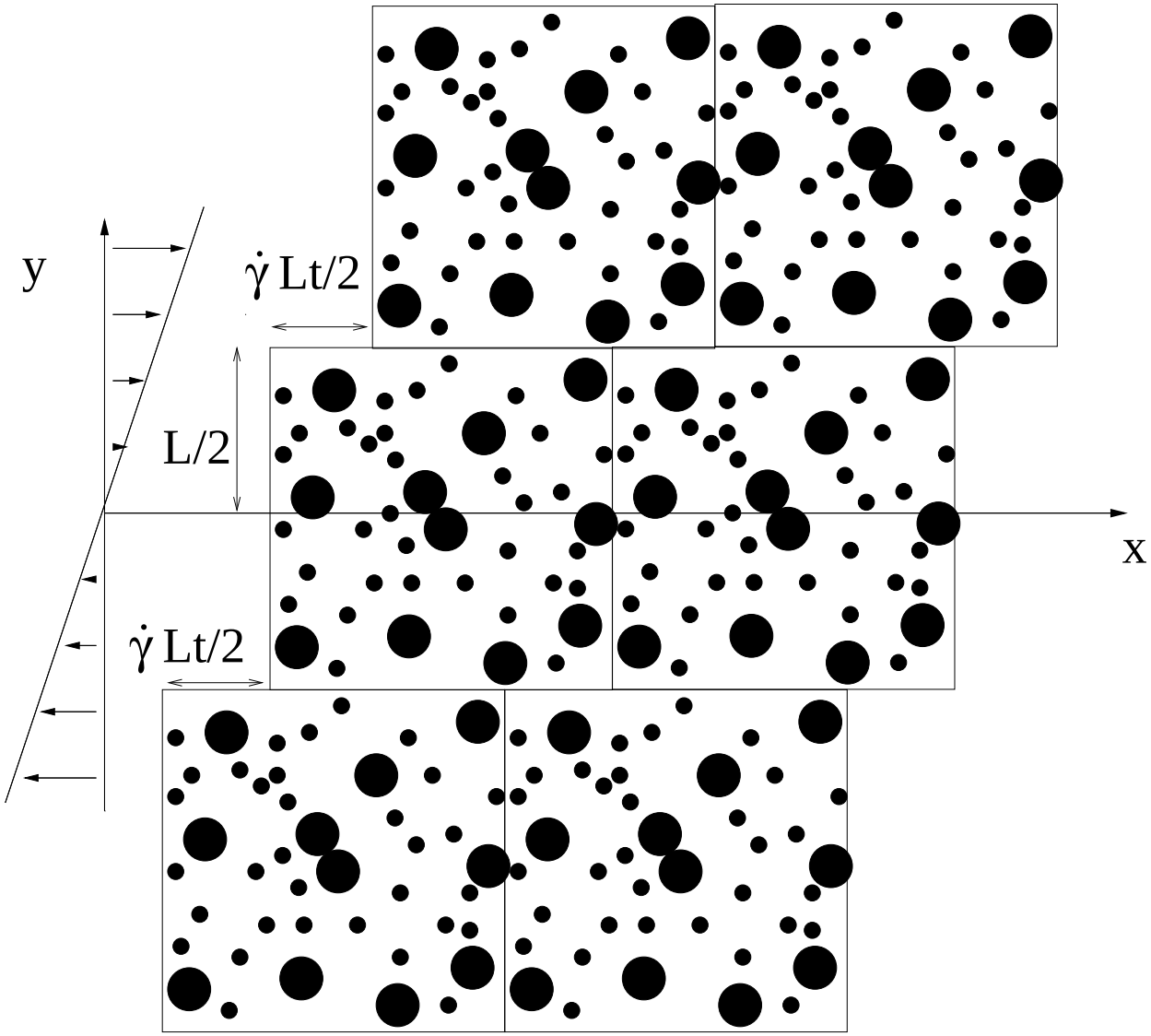

FIG. 1.

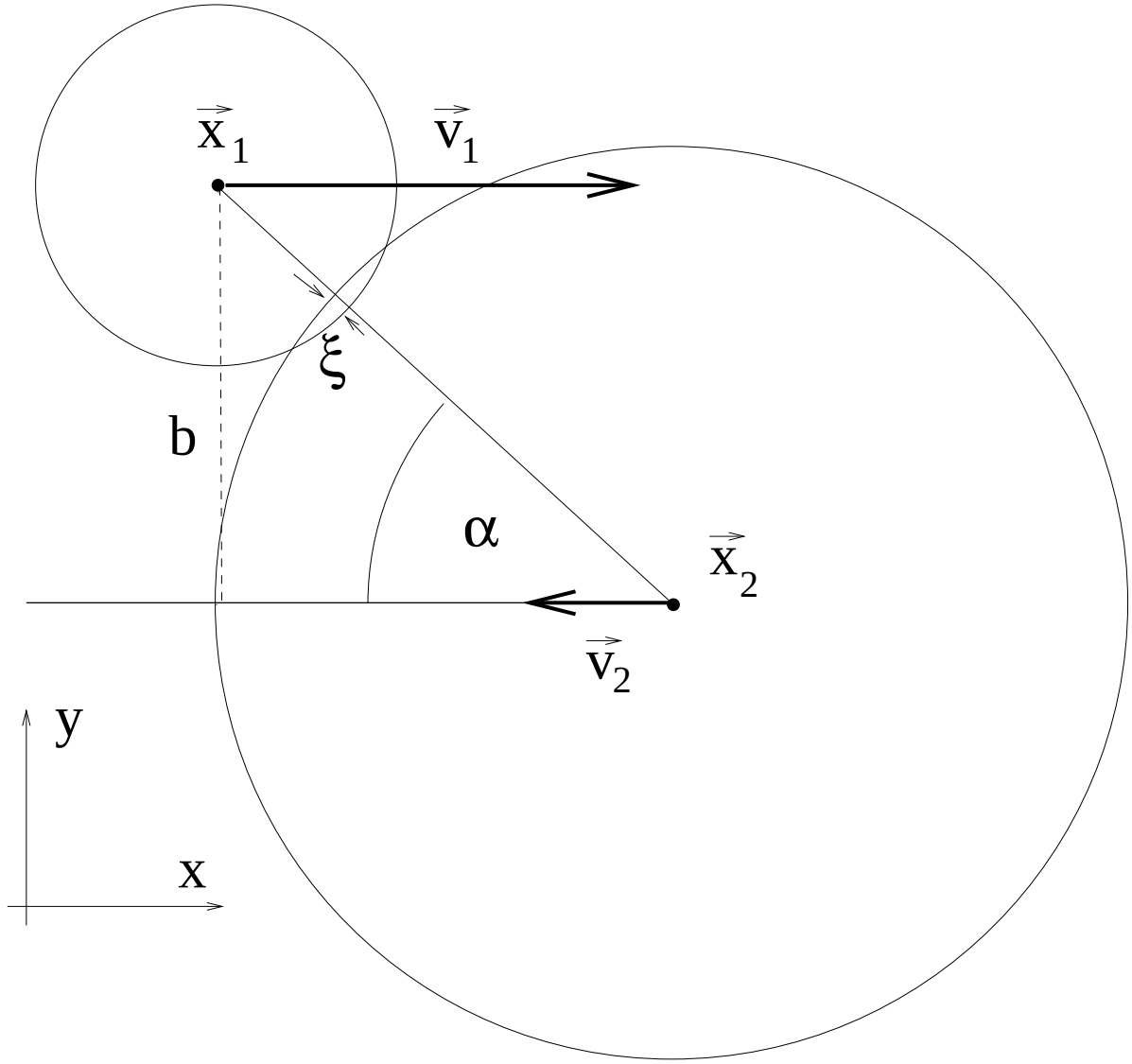

FIG. 2.

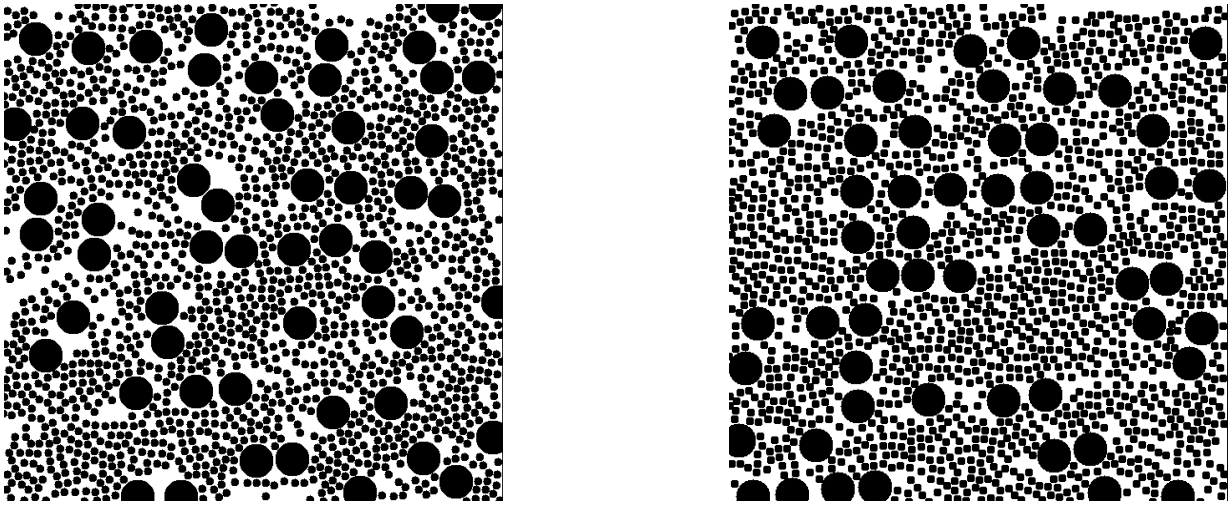

(a) (b)

FIG. 3.

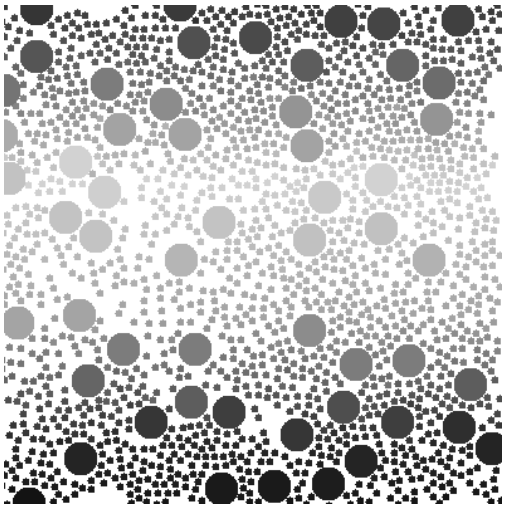

(a)

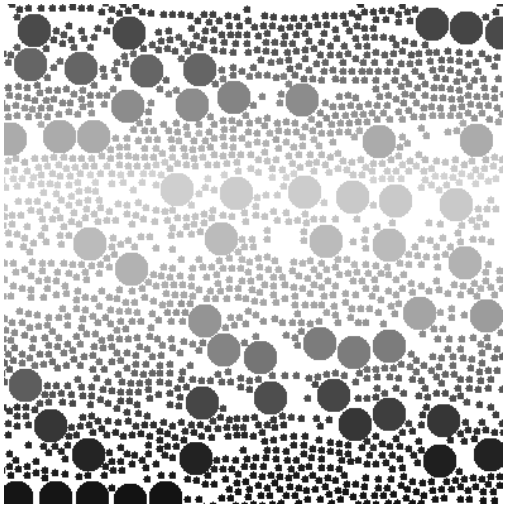

(b)

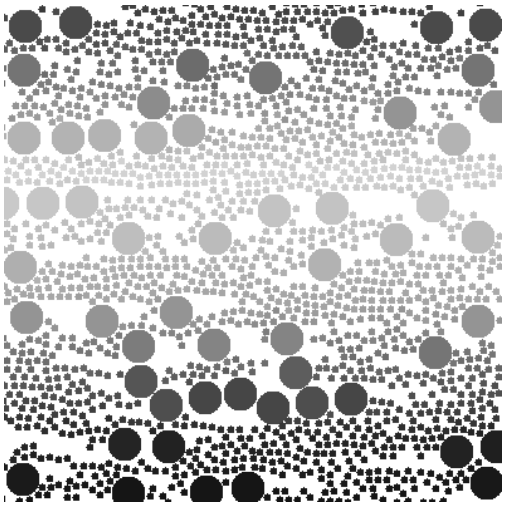

(c)

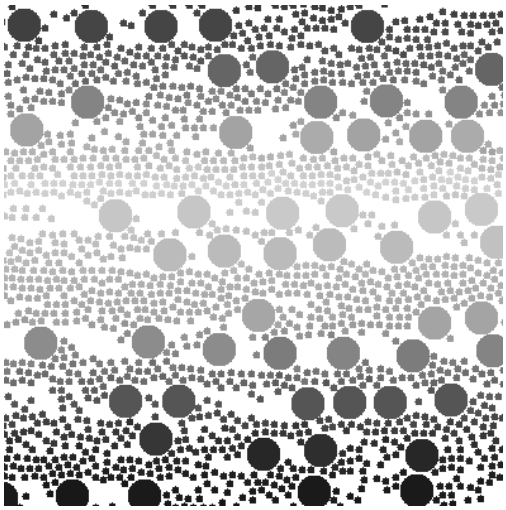

(d)

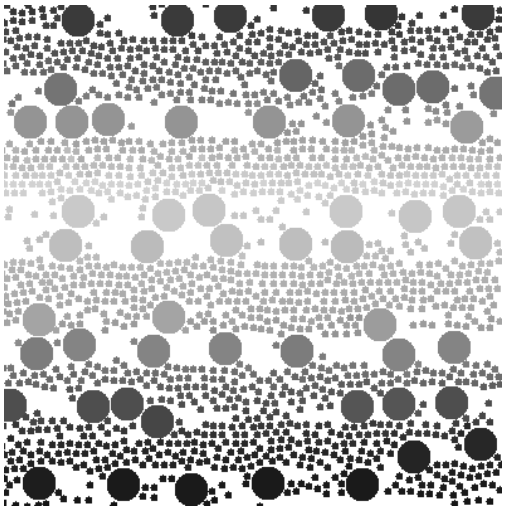

(e)

FIG. 4.

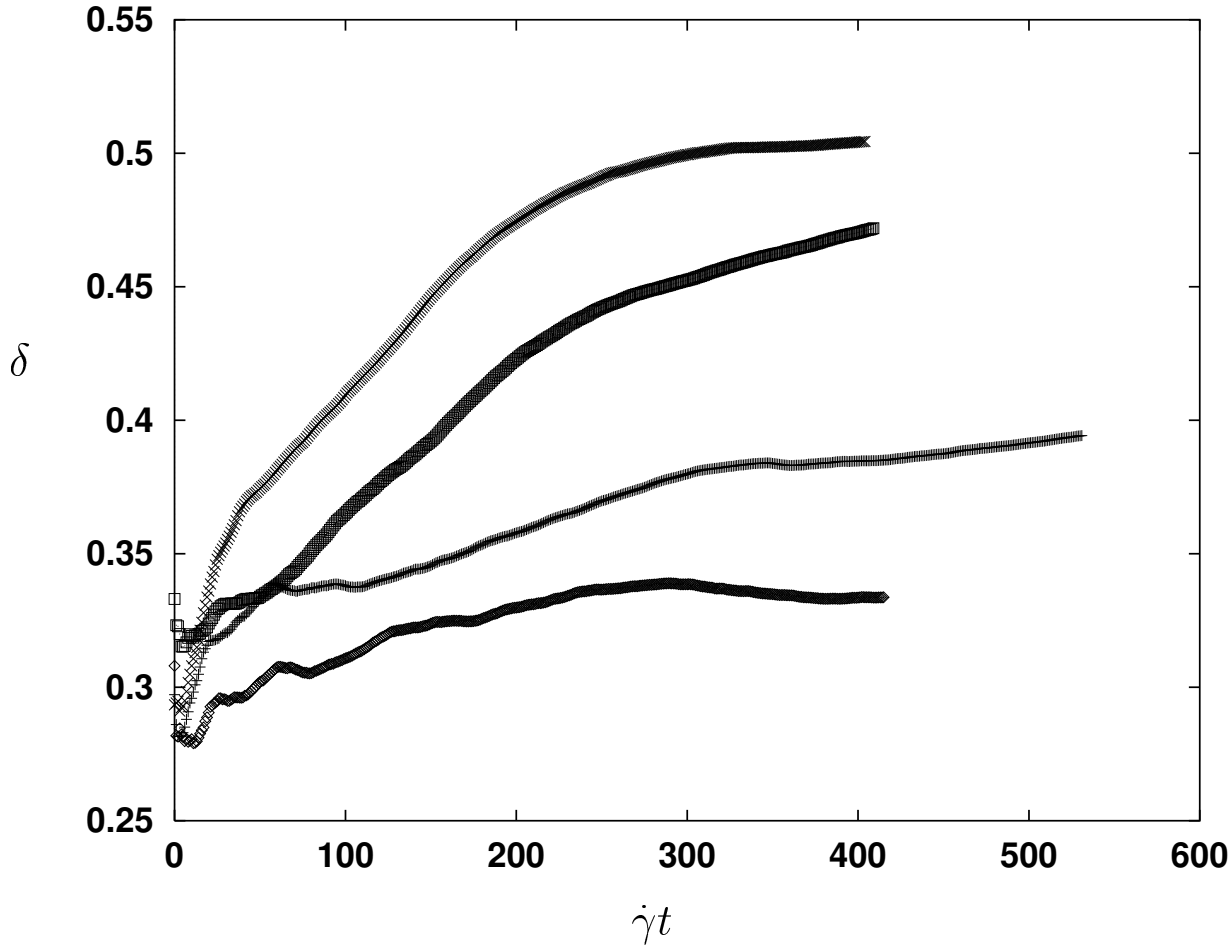
0.55
0.5
0.45
0.4
0.35
0.3
0.25
δ
0
100
200
300
400
500
600
$\dot{\gamma}t$

FIG. 5.

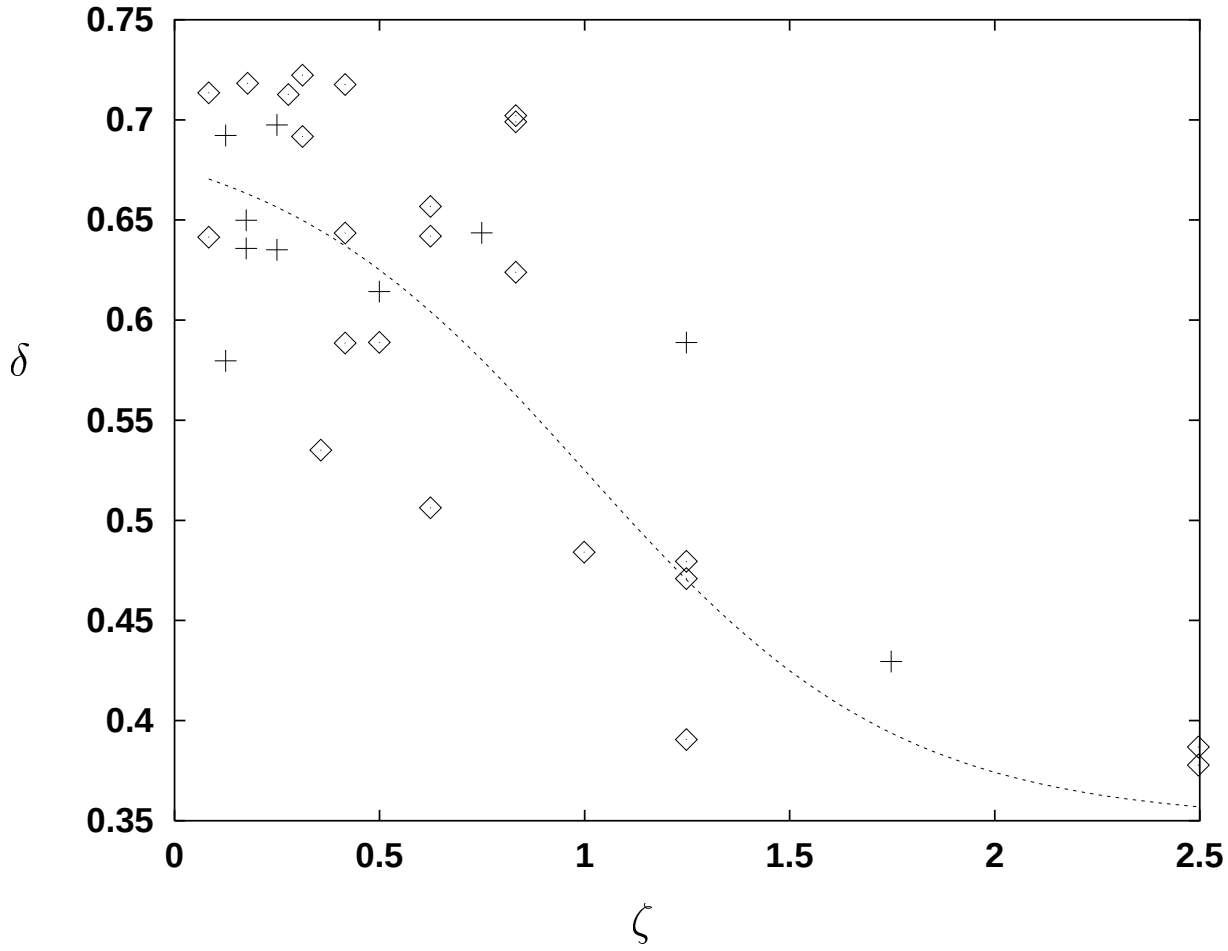

FIG. 6.

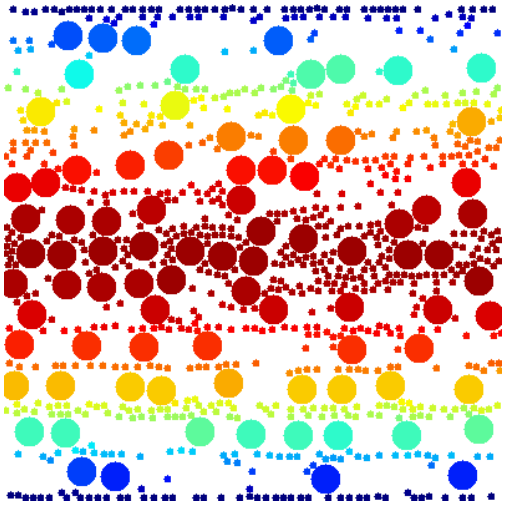

(a)

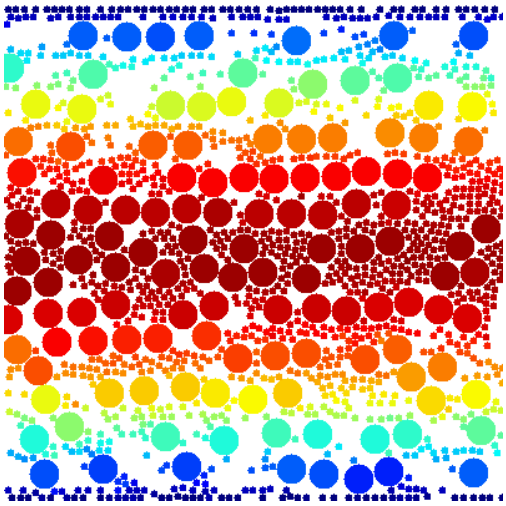

(b)

FIG. 7.

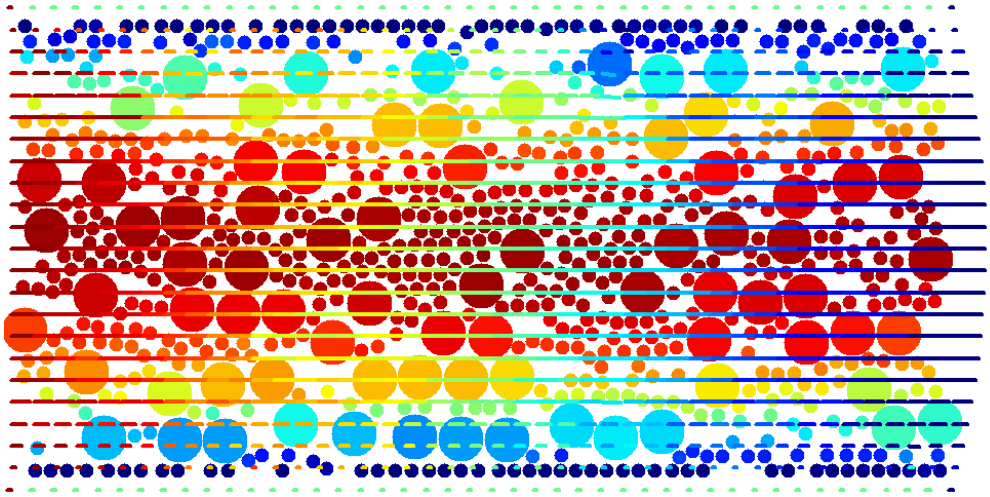

FIG. 8.

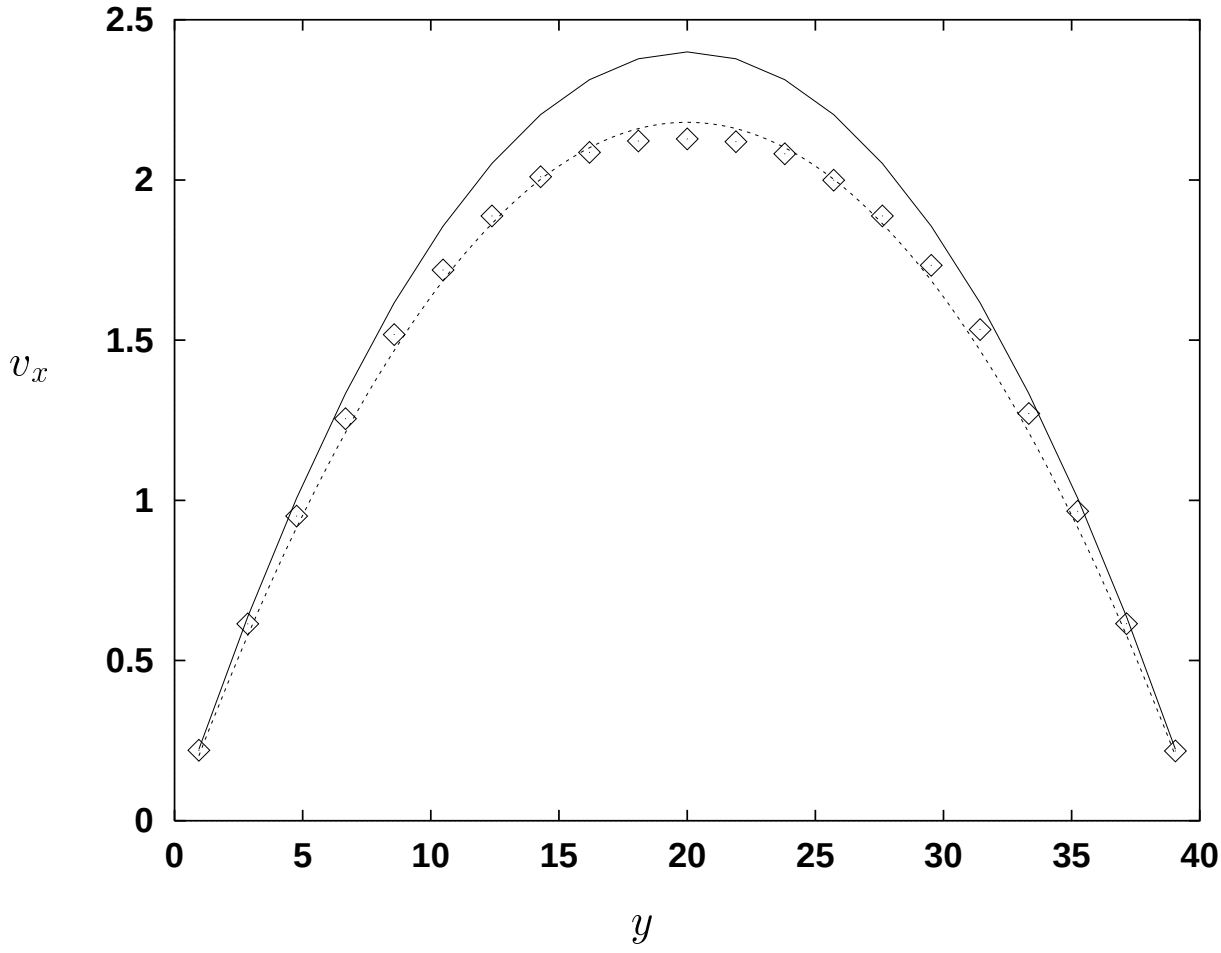

FIG. 9.